

Experimental Research on Pulse Electroforming of Ni-Co Alloy with Dual Anodes

Xinfeng Fu¹, Shuangqing Qian^{1,*}, Yong Zhang², Xiaofeng Wan¹, Jingling Zhou¹, Hua Zhang¹

¹ School of Mechanical Engineering, Nantong University, Nantong 226019, China

² Department of mechanical and electrical engineering, Shazhou Institute of Technology, Zhangjiagang 215600, China

*E-mail: sqqian@ntu.edu.cn

Received: 5 March 2022 / Accepted: 24 April 2022 / Published: 7 May 2022

Ni-Co alloy is widely used in industry due to its excellent properties. In this paper, based on the sulfamate system, dual anodes are used to get Ni-Co alloy by electroforming. The effects of current density and pulse parameters on the microhardness, composition and surface microstructure of electroformed Ni-Co alloy are investigated and analysed by hardness tester, energy spectrometer (EDS) and scanning electron microscopy (SEM). The experimental results show that the current density and pulse parameters have significant impact on the performance of the electroformed layer, and it is determined that the current density of 2A/dm², the frequency of 5kHz, and the duty cycle of 30% are the best parameters electroforming Ni-Co alloy with dual anodes.

Keyword: Electroforming, Dual anodes, Ni-Co Alloy

1. INTRODUCTION

In recent years, alloys have excellent properties such as high temperature resistance and corrosion resistance, which can play an important role in infrastructure and surface decoration. Therefore, Ni-Co alloy have been extensively studied by experts and scholars [1-3]. Ni-Co alloy also has obvious advantages in terms of wear resistance, magnetic properties and high hardness, which has been widely used in industry as a crucial material [4-6].

Nano Ni-Co alloy also has been widely studied in recent years due to its excellent properties which has been applied in many fields [7,8]. Hang [9] successfully synthesized Ni-Co alloy nanocones arrays by a one-step electrodeposition method. Wu [10] applied nanoscale Ni-Co alloy to sensitive nonenzymatic glucose sensors because they can provide excellent electrical conductivity and high active surface area. Li [11] prepared Ni-Co phosphate bimetallic nanostructures on nickel foam surface for composite supercapacitors.

There were many methods for preparing Ni-Co alloy, such as chemical vapor deposition, physical vapor deposition [12,13]. Many new techniques have also been used to synthesize Ni-Co alloy substrates, including electrodeposition, microemulsions, sol-gel methods, and magnetically induced carbonylation [14,15]. Compared with the traditional metal processing technology, electroforming Ni-Co alloy have the advantages of economy and simple setup under the same working environment, reducing the number of machining times from blanks to parts, and improving the machining accuracy of parts [16-18]. Ni-Co alloy can be prepared with a variety of electroforming solutions, such as sulfate systems, sulfamate systems, etc. The sulfamate system can obtain coatings with lower stress than other systems [19,20]. Whereas, problems such as cathodic polarization and hydrogen evolution also occur in the process of electroforming Ni-Co alloy. Cathodic polarization affects the adhesion of metal ions and also affects the uniform distribution of metal on the cathode surface. The main problem in the Ni-Co alloy electrodeposition process was the hydrogen evolution reaction, which reduces the current density and leads to the deposition of metal ions on the anode [21-23]. Based on the problems existing in the preparation of Ni-Co alloy by electroforming technology, many scholars have made some attempts to improve the surface quality of the electroforming layer.

To improve the effect of cathodic polarization and hydrogen evolution reaction on electroformed layers, Lupi [24] added sodium lauryl sulfate and saccharin to the bath to improve the hydrogen evolution reaction. Karpuz [25] used electroforming solutions containing different cobalt content to electroform Ni-Co alloy. The experimental results showed that the cobalt content has a significant effect on the alloys structure, magnetic properties and magnetorheological properties. The properties of electroformed layers can be improved by the study of assisted electroforming. Su [26] experimentally verified that the electroformed layer obtained by using supercritical carbon dioxide assisted electroforming of Ni-Co alloy has higher hardness and dense microstructure. Akshatha R [27] used ultrasonic induced electroforming of Ni-Co alloy in order to improve the corrosion resistance of Ni-Co alloy. The experimental results proved that ultrasonic induction can significantly improve the corrosion resistance of the coating. Zhang [28] investigated titanium nitride nanoparticles to enhance the wear resistance of electroformed layers, the dense structure of the Ni-Co alloy layer prepared with the aid of titanium nitride nanoparticles was demonstrated.

In addition, changing the power source to improve the coating properties has been increasingly investigated by scholars. Many scholars have studied and compared the effects of DC current and pulsed current on electroformed layers, and experimentally verified that the pulse parameters affect the surface morphology and microstructure of electroformed layers. Vazquez-Arenas [29] prepared Ni-Co alloy under DC pulse and pulse reverse plating conditions, respectively. Studies have shown that the electroformed layer obtained by changing the pulse parameters was smoother. Chung [30] investigated the effects of pulse frequency and current density on the nanomechanical properties of electrodeposited Ni-Co alloy. It was shown that the coating surface was smoother with lower current densities and higher pulse frequencies. Vikash [31] verified the effect of pulse electroforming on the electroformed layer through experiments, and the experimental results also proved that pulse electroforming can obtain more uniform and smooth electroformed layer.

The reaction principle of electroforming with a single anode, as shown in **Fig. 1(a)** is difficult to control the content of cobalt in the solution during electroforming. As electroforming continues, cobalt

ions need to be added in the solution to keep the cobalt ion concentration constant. As shown in **Fig. 1(b)**, the method of electroforming Ni-Co alloy used dual anodes is proposed in this paper which can ensure the stability of cobalt ions. The effects of current density and pulse parameters on Ni-Co alloy are thoroughly studied. The optimal parameters of dual anodes electroforming Ni-Co alloy with better microstructure are determined.

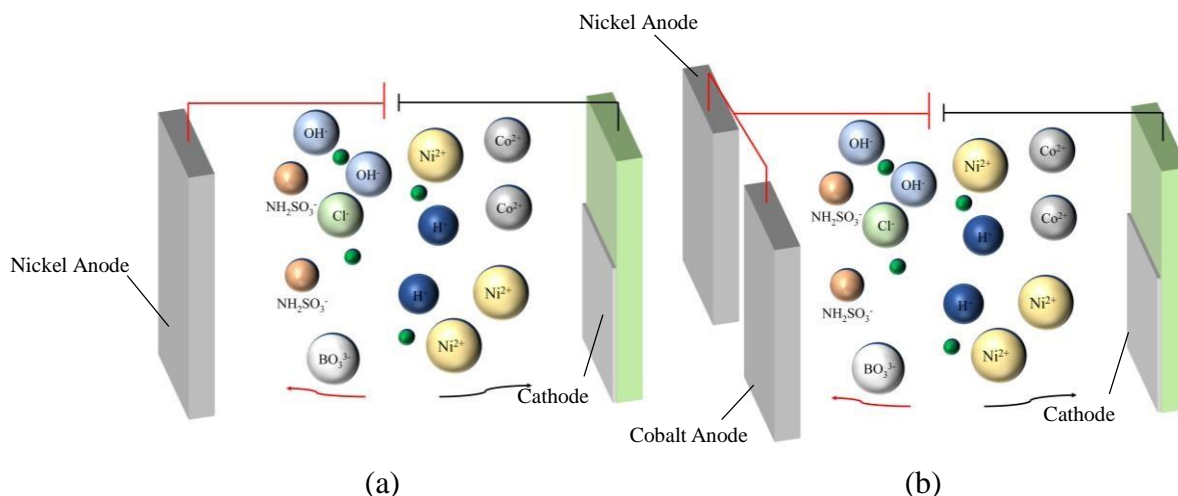


Figure 1. (a) Schematic diagram of single anode reaction (b) Dual anodes reaction principle diagram

2. EXPERIMENTAL METHODS

2.1 Preparation method

Due to the excellent performance of the electroformed layer obtained by the sulfamate system, the sulfamate system is used in this experiment. The output signal of the pulse power used during the experiment is square wave which is shown in **Fig. 2**, the pulse frequency and duty cycle are calculated by the following equations:

$$D = \frac{T_1}{T} \tag{1}$$

$$f = \frac{1}{T} \tag{2}$$

- in the formula: f — Pulse frequency
 D — Duty Cycle
 T — Pulse duration
 T_1 — High level duration

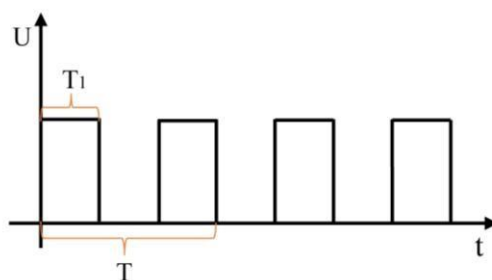


Figure 2 Output waveform of the pulse power supply used in the experiment

The composition and the electroforming process conditions of Ni-Co plating solution are shown in **Table 1**. The solution used in the experiment is composed of analytical grade chemicals and prepared with deionized water. The pH of the electroforming solution is measured by a pH meter and adjusted to a suitable value using H_3BO_3 . The prepared solution is precipitated for 24 hours and filtered prior to use.

Table 1. Electrolyte composition and electrodeposition conditions

Bath constituent or electrodeposition conditions	Amount or conditions
Nickel sulfamate	400 g/L
Cobalt sulfamate	40 g/L
Boronic acid	30 g/L
Nickel chloride	15 g/L
Sodium dodecyl sulfate	1-2 g/L
Average current density	1, 2, 3, 4 A/dm ²
Duty cycle	20%, 30%, 40%, 50%
Frequency	2, 3, 4, 5 kHz
Temperature	45 °C
pH	4-5

2.2 Electroforming experimental equipment

The electroforming equipment is self-designed as shown in **Fig. 3**. In this set of equipment, the power supply, two anode plates, cathode plates, electroforming tank, electroforming liquid circulation system and temperature controller constitute the electroforming system. The temperature controller keeps the solution temperature constant during the experiment. The water circulation system consists of flowmeter, ball valve, filter, pump and overflow valve. The two anodes need to be kept at an appropriate

distance from the cathode. In this experiment, in order to deposit nickel and cobalt on the cathode better, the distance between cathode and anode is 60mm.

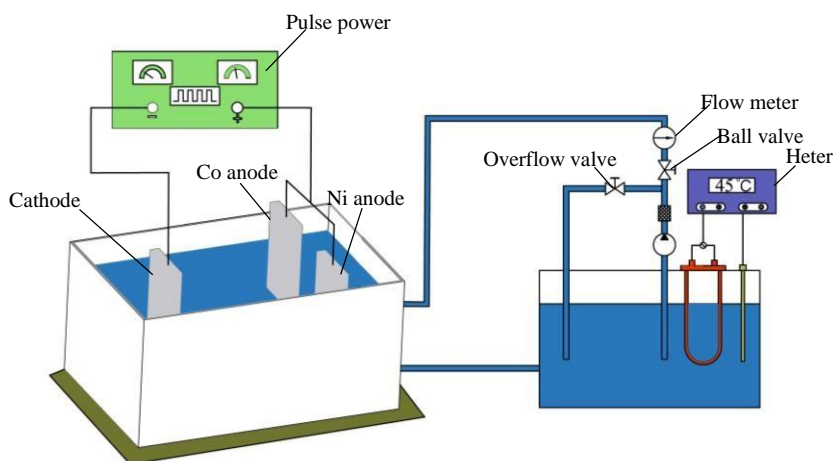


Figure 3. Simple installation diagram of experimental equipment

Many shapes of cathodes can be manufactured by 3D printing without touching tools, and 3D printed cathodes have the advantages of lower cost and easier demoulding compared to other material cathodes. Therefore, 3D printed cathodes are used in this paper [32]. The cathode substrate is divided into three parts, namely the clamping area, the insulating area and the electroforming area. The cathode material is photosensitive resin, which is made by stereolithography equipment. The surface of the cathode substrate is coated with commercial silver conductive paint (MECHANIC Supplies) for conducting electricity which is shown in **Fig. 4**.



Figure 4. physical view of cathode substrate

2.3 Electroforming preparation

In the experiment, two anodes, one is 99.99% pure nickel plate and the other is 99.99% pure cobalt plate. In order to ensure the quality of electroforming layer, the cathode surface is polished and pickled before the experiment. The two anodes in the electroforming tank are placed in parallel. Before the experiment, both anodes need to be polished, degreased, acid-washed and cleaned with deionized water. After the completion of electroforming, the obtained samples are placed in acetone solution then

ultrasonic waves are used to help dissolve the substrate in order to obtain the complete electroformed layer.

3. RESULTS AND DISCUSSION

This experiment investigated the surface morphology and microhardness of the Ni-Co casting layer under the conditions of the dual anodes electroforming process. The temperature and pH of the solution are kept constant at 45°C and 4.5 during the experiments.

3.1. Influence of Pulse current density on electroformed layer

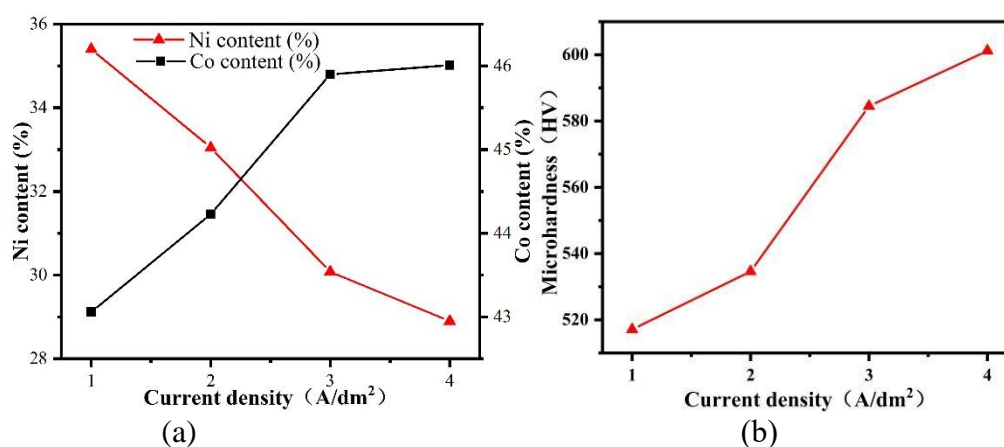


Figure 5. Effect of current density on the composition and microhardness of Ni-Co alloy cast layers (a) Trend of Ni and Co content (b) Microhardness

To investigate the effect of current density on nickel and cobalt content under the dual anode system, their trends are presented in **Fig. 5(a)**. The experiments are conducted with the pulse power output frequency of 5 kHz and the duty cycle of 50% constant, and the current density is increases from 1A/dm² to 4A/dm². The on and off time of current is kept constant under a certain pulse frequency and duty cycle condition. With the increase of current density from 1A/dm² to 4A/dm², the cobalt content in the cast layer gradually increases, and it can be obtained that the increase of current density is beneficial to the deposition of cobalt. In contrast to the trend of cobalt content, nickel content gradually decreases. The microhardness of the electroformed layer gradually increases with the increase of current density as shown in **Fig. 5(b)**. These results are in agreement with the reports by Hu [33] and Wu [34], which indicated that as the cobalt content in the cast layer of the nickel-cobalt alloy increases, the microhardness also increases. The microhardness of the electroformed layer is reached the highest value of 601.2 HV.

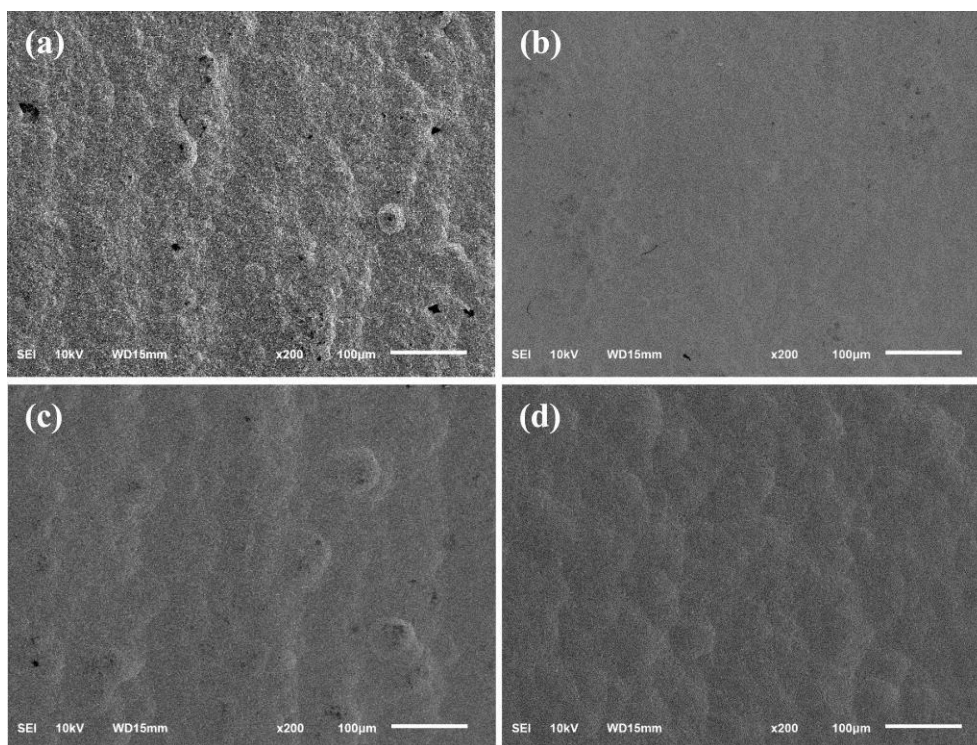


Figure 6. SEM micrographs showing the effect of pulsed current density on the surface morphology of Ni-Co alloy (a)1 A/dm² (b)2 A/dm² (c)3 A/dm² (d)4 A/dm²

Fig. 6 shows the SEM micrographs of the Ni-Co electroformed layer surface obtained at pulse current densities of 1, 2, 3, and 4A/dm², respectively. The results shows that the surface of the electroformed layer become smoother and the grain size become finer when the pulse average current density increases from 1 A/dm² to 2 A/dm². When the pulse average current density rises to 4 A/dm², the grains of the Ni-Co electroformed layer begin to grow and the surface of the electroformed layer become rough. Properly increasing the cathode current density could increase the overpotential, promoted the nucleation rate of the crystal grains and achieve the effect of grain refinement. The similar report made by Hu [33] as the pulse current density increases, the grains of Ni-Co alloy layer become rougher and coarser.

3.2. The influence of pulse frequency on electroformed layer

The surface morphology of copper electrodeposits obtained at 2, 3, 4, and 5kHz pulse frequencies which is demonstrates in **Fig. 7**. Other parameters are kept constant (the current density of 3A/dm² and the duty cycle of 50%). When the frequency is improved to 5kHz, the surface of the Ni-Co casting layer is smoothest and most uniform. The experiments results made by Gao [35] show with the increase of pulse frequency, the surface of the cast layer becomes smoother, the organization is denser, and the grain is refined. The analysis results shown that with the gradual increase of pulse frequency, the time of pulse period, energization and Ni-Co deposition within one pulse cycle are shortened. the growth of the original grains is interrupted and new grains are grown.

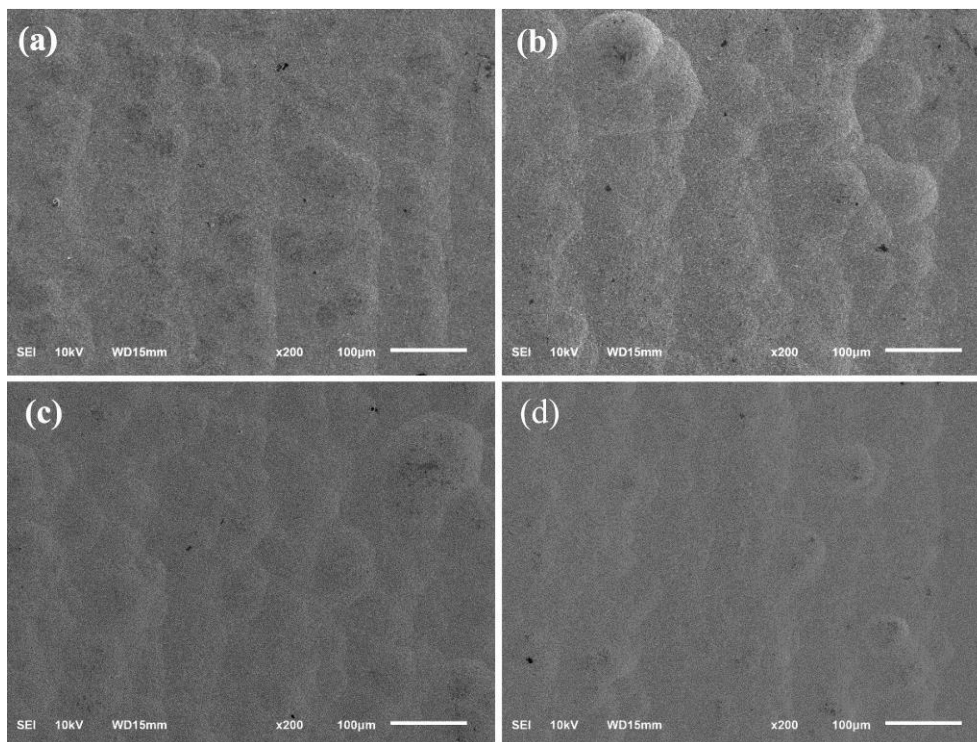


Figure 7. SEM micrographs showing the effect of pulse frequency on the surface morphology of Ni-Co alloy. (a) 2kHz. (b) 3kHz. (c) 4kHz. (d) 5kHz

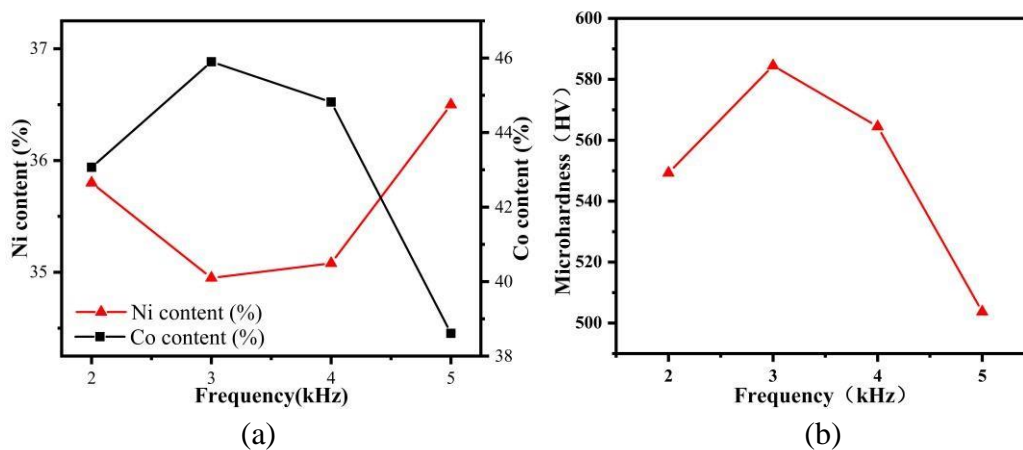


Figure 8. Effect of frequency on the composition and microhardness of Ni-Co alloy cast layers (a) Trend of Ni and Co content (b) Microhardness

The influence of pulse frequency on nickel and cobalt content in the cast layer is illustrated in **Fig. 8(a)**. It can be seen that with the increase of pulse frequency, the cobalt content in the electroformed layer shown a trend of increase first and then decrease, reached the highest peak at the frequency of 3kHz. On the contrary, the nickel content decreases first and then increases. The same trend as the change of cobalt content in the cast layer, the microhardness of the electroformed layer also shown a trend of increase first and then decrease which is shown in **Fig. 8(b)**. In the frequency of 3 kHz, when the cobalt content reaches its maximum value, the microhardness value also reached its maximum which is 584.5 HV.

3.3 The influence of duty cycle on electroforming layer

The surface morphology of the electroformed layer achieved with different duty cycles which is depicts in **Fig. 9**. The Ni-Co electrodeposition is obtained from an average current density of 3 A/dm^2 and the frequency of 5kHz. When the duty cycle is 30%, the electroformed layer obtained is the most uniform and smoothest with fewer defects. The experimental results proved that when the duty cycle is increased to 30%, a more uniform Ni-Co electroforming layer with good surface quality can be obtained. When the duty cycle exceeds 30%, the deposition time of nickel and cobalt will increase. The continuous grain growth time within each pulse cycle will increase and the surface of the electroformed layer would become rough. This result is in agreement with the reports by Subramanian [36], which reports smooth Ni-Co alloy cast layer can be obtained at lower duty cycle.

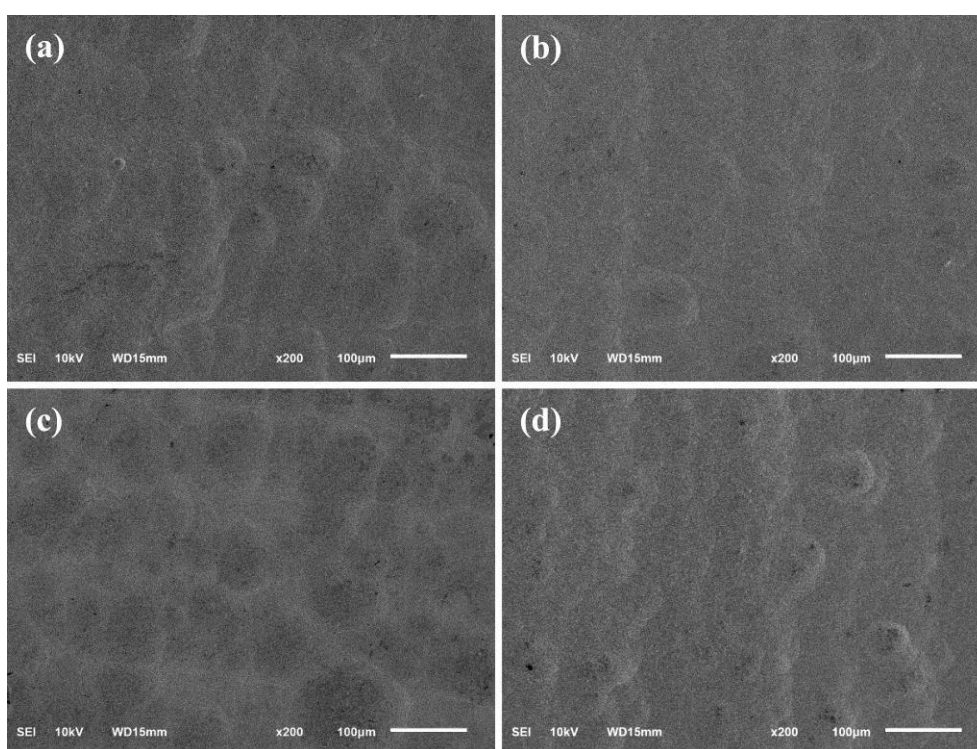


Figure 9. SEM micrographs showing the effect of the duty cycle on the surface morphology of Ni-Co alloy. (a) 20%. (b) 30%. (c) 40%. (d) 50%

Fig. 10(a) shows the nickel and cobalt content in the electroformed layer. It can be learned that when the duty cycle increases from 20% to 50%, the content of cobalt in the electroformed layer gradually increases and reached the maximum value at the duty cycle of 50%, however, the nickel content shows an opposite trend. When the content of cobalt in the electroformed layer increases gradually with the duty cycle, the microhardness of the electroformed layer also gradually increases and reached the maximum value of 597 HV at the 50% duty cycle as shown in **Fig. 10(b)**. These results are agreed with the reports by Subramanian [36] and Yu [37], which both indicated that the Co content in the casting layer increases as the growth of duty cycle in the pulse electrodeposition. Meanwhile, the microhardness of the cast layer increases with the increase of duty cycle.

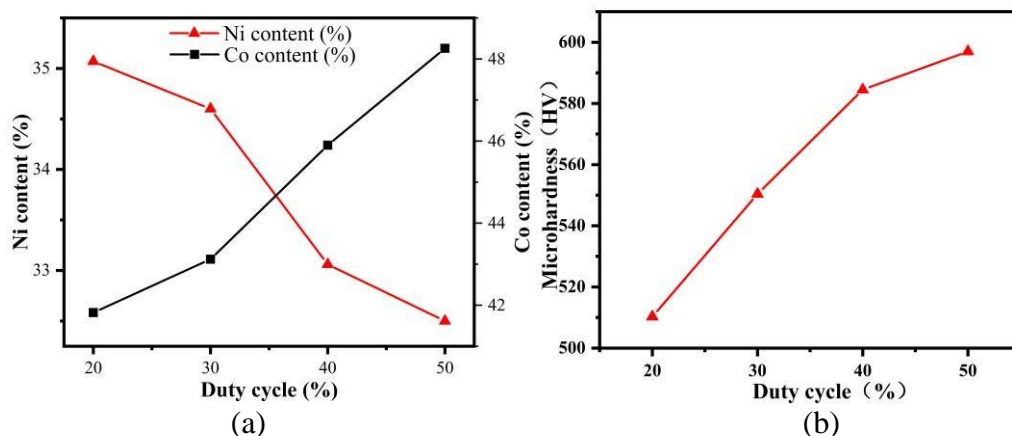


Figure 10. Effect of duty cycle on the composition and microhardness of Ni-Co alloy cast layers (a) Trend of Ni and Co content (b) Microhardness

4. CONCLUSIONS

In this experimental study, in order to obtain Ni-Co electroformed layers with high uniformity and quality, the dual anodes system was used for the electrodeposition experiments of Ni-Co alloy at different current densities and pulse parameters. The effects of current density, duty cycle and frequency on the microstructure, microhardness and cobalt content of the Ni-Co electroformed layers were investigated. The results are as follows:

(1) By experimental analysis, the content of cobalt in the deposited layer gradually increases with the increase of the average current density, and the microhardness also gradually increases. Meanwhile, with the increase of current density, the grains of nickel-cobalt deposited layer are firstly refined and then become coarser.

(2) With the increase of pulse frequency, the cobalt content and microhardness in the deposited layer increase first and then decrease. Meanwhile, in a certain range, deposited layer with good surface quality can be obtained with the increase of pulse frequency.

(3) The experimental results prove that with the increase of duty cycle, the cobalt content in the deposited layer tends to rise and the microhardness increases gradually. In a certain range, the surface quality of the deposited layer is more excellent with the increase of duty cycle, however while the duty cycle is too high, the deposition time in a single pulse cycle increases and the interruption event is shortened, which will reduce the surface quality of the electroformed layer.

ACKNOWLEDGMENTS

We gratefully acknowledged the Nantong Basic Science Research Program: Basic Research on Processing Technology of Microgroove Heat Pipe Absorption Core Based on 3D Printing (No: JC2021064).

References

1. D. Farkas, *J Mater Sci.*, 55(2020)9173.
2. X. Lu, C. Dong, X. Guo, J. Ren, H. Xue, F. Tang, Y. Ding, *J Mater Res Technol.*, 158(2020)76.
3. H.Z. Li, M. Kang, Y. Zhang, Y.T. Liu, M.F. Jin, Samuel Nyambura Mbugua, G. Zhu, C.H. Liu, *Nanosci Nanotechnol Lett.*, 11(2019)47.
4. L. Tian, J. Xu, S. Xiao, *Vacuum*, 86(2019)27.
5. R. Radadi, M. Ibrahim, *Korean J Chem Eng.*, 37(2019)1599.
6. Y.F. Yang, B. Deng, Z.H. Wen, *Adv Chem Eng Sci.*, 1(2011)27.
7. W.R. Li, J.J. Hao, W. Liu, S.H. Mu, *J Alloys Compd.*, 853(2021).
8. J. Kong, M. Sabatini, L. Monaco, J. Tam, U. Erb, *J Mater Sci.*, 56(2021)1749.
9. N. Wang, T. Hang, S. Shanmugam, M. Li, *CrystEngComm.*, 16(2014)6937.
10. D. Wu, Z. Zou, X. Lu, K. Guo, N. Yang, C. Xu, *J Mater Sci.*, 54(2019)10695.
11. L. Min, Y.Y. Luo, J. Chen, Q.K. Zhang, G.X. Luo, L.B. Zhao, Z.D. Jiang, *J Alloys Compd.*, 893(2021).
12. R. Radadi, M. Ibrahim, *Korean J Chem Eng.*, 38(2020)152.
13. I. Khazi, U. Mescheder, J. Wilde, *Materials*, 14(2021)14.
14. X. Shen, K. Cao, J. Zhou, *T Nonferr Metal Soc.*, 16(2006)1003.
15. D.Y. Feng, H. Yang, Q.X. Wang, X.Z. Guo, *J Mater Sci.*, 54(2019)4719.
16. I. Khazi, U. Mescheder, *Mater Res Express*, 6(2019)8.
17. X.F. Zhan, Q.D. Cao, K. Trieu, X.P. Zhang, *J Mater Eng Perform.*, 29(2020)1741.
18. R. Sekar, K.K. Jagadesh, G.N.K. Bapu, *T Nonferrous Metal Soc China*, 25(2015)1961.
19. L.C. Rudnik, *Hydrometallurgy*, 54(2000)133.
20. M. Srivastava, V.E. Selvi, V.K.W. Grips, K.S. Rajam, *Surf Coat Tech.*, 201(2006)3051.
21. P.M. Ming, D. Zhu, Y.Y. Hu, Y.B. Zeng, *Vacuum*, 83(2009)1191.
22. Y.M. Byoun, Y.T. Noh, Y.G. Kim, S.H. Ma, G.H. Kim, *J Nanosci Nanotechnol.*, 18(2018)2104.
23. Z. Li, Z. Duan, H. Liu, *Int Conference on Inform Comput Appl.*, 308(2012)685.
24. C. Lupi, D. Pilone, *Miner Eng.*, 14(2001)1403.
25. A. Karpuz, H. Kockar, M. Alper, O. Karaagac, M. Hacıismailoglu, *Appl Surf Sci.*, 258(2012)4005.
26. C. Liu, F. Su, J. Liang, *Surf Coat Tech.*, 292(2016)37.
27. S. Akshatha R, A. Chitharanjan Hegde *Surf Coat Tech.*, 322(2017)99.
28. W.W. Zhang, S.S. Du, B.S. Li, T.Y. Mei, J.J. Wang, *J Alloys Compd.*, 865(2021).
29. J. Vazquez-Arenas, T. Treeratanaphitak, M. Pritzker, *Electrochim Acta*, 62(2012)63.
30. C.K. Chung, W.T. Chang, *Thin Solid Films*, 517(2009)4800.
31. V.K. Sharma, N. Kukreja, K. Mausam, *Mater Today Proc.*, 45(2021)3449.
32. Y.Y. Wu, S.Q. Qian, H. Zhang, Y. Zhang, H. Cao, M. Huang, *Micromachines*, 10(2019)12.
33. X.Y. Hua, N.S. Qu, *Thin Solid Films*, 679(2019)110.
34. Z.W. Wu, Y.P. Lei, Y. Wang, H.G. Fu, *Materialwiss Werkstofftech*, 44(2013)593.
35. J.C. Gao, H.M. Jin, J.Q. Zhang, J. Shi, L. Li, *Appl Mech Mater.*, 84(2011)86.
36. M. Subramanian, N. Dhanikaivelu, R. Rama Prabha, *Trans IMF*, 85(2007)274.
37. M.M. Yu, H.Y. Li, Y. Wang, *Adv Mater Res.*, 602(2013)565.